Detecting response of microelectromechanical resonators by microwave reflectometry

Bernard Legrand, D. Ducatteau, D. Theron, B. Walter, H. Tanbakuchi

Detecting response of microelectromechanical resonators by microwave reflectometry

Cite as: Appl. Phys. Lett. **103**, 053124 (2013); https://doi.org/10.1063/1.4817411
Submitted: 31 October 2012 • Accepted: 19 July 2013 • Published Online: 02 August 2013

B. Legrand, D. Ducatteau, D. Théron, et al.

Detecting response of microelectromechanical resonators by microwave reflectometry

B. Legrand,[1] D. Ducatteau,[1] D. Théron,[1] B. Walter,[1] and H. Tanbakuchi[2]
[1]*Institut d'Electronique, de Microélectronique et de Nanotechnologie, IEMN-CNRS UMR 8520, 59652 Villeneuve d'Ascq, France*
[2]*Agilent Technologies, 1400 Fountaingrove Parkway, Santa Rosa, California 95403, USA*

(Received 31 October 2012; accepted 19 July 2013; published online 2 August 2013)

Microwave reflectometry is proposed as an effective technique to detect the vibration of capacitively transduced microelectromechanical resonators. The transducer capacitor is probed by an incident wave, which is reflected being modulated by the time variations of the resonator displacement. Calculations demonstrate that the sensitivity of the technique is maximum for a given microwave frequency depending on the transducer total capacitance. Experimental data show that capacitance variations as low as 3 zF/$\sqrt{}$Hz are measurable at 4 GHz for the studied devices. Such a performance corresponds to a sub-picometer resolution in vibration amplitude of the microelectromechanical resonator. The measurement technique is particularly appropriate for resonant sensors when high signal-to-noise ratio and fully electrical detection are required. It can be used for device resonance frequency up to several hundreds of MHz. © *2013 AIP Publishing LLC*.
[http://dx.doi.org/10.1063/1.4817411]

MicroElectroMechanical Systems (MEMS) have given rise in the last decades to numerous products, particularly in the field of sensors and actuators.[1–5] Micro-resonators are MEMS devices that transpose in the electrical domain the characteristics of a microscale mechanical resonance.[6] Applications concern devices for signal processing like filters and time references,[7–9] but also vibrating sensors,[10,11] the resonance characteristics being sensitive to external interactions. Many academic and industrial research works have been carried out especially in the field of mass sensing[12,13] and label free detection for biochemical applications,[14–16] but also in the field of force sensors like Atomic Force Microscopy probes.[17,18] Various physical principles may be used to assure electromechanical transduction performed by the MEMS resonators.[10,19] Among them, the capacitive one is widely employed because it is easily integrated with the mechanical parts and has benefited since the 1980s from surface micromachining processes compatible with silicon integrated circuit technologies.[6,14] The mechanical vibration is simply detected through the output current flowing from the time varying capacitance of the MEMS resonator transducer when a voltage is applied. However, capacitive transducers generally have two drawbacks, as MEMS resonators are downsized to reach higher frequencies, typically above 10 MHz. First, capacitive transducers present electrical impedance of several kilo-ohms that significantly exceeds the 50 Ω standard.[20] Second, they have parasitic input/output coupling capacitance. Therefore, the measured signal from a capacitive transducer is generally weak and superimposed with a parasitic signal floor, which may mask the desired mechanical resonance signal. The impedance mismatch between the MEMS resonator and the 50 Ω measurement set-up, leading in particular to poor signal-to-noise ratio (SNR), negates much of the benefit that would be otherwise attained from optimal sensitivity and measurement dynamic. Various strategies have been deployed to circumvent these difficulties. Differential measurement schemes or frequency mixing techniques[21] have been widely used to reject the capacitive crosstalk. Passive impedance matching networks[22] or integrated amplifiers[14,23] are also commonly used for improving the sensitivity and SNR. Such techniques require specific circuit design depending on the MEMS resonator. They are often band-limited, and matching elements need to be placed in the vicinity of, or integrated with the MEMS resonator. As a consequence, they are not appropriate for all circumstances, especially when low-cost and disposable vibrating sensor products are concerned, or when probing multiple resonance modes over a wide frequency band is desired. In this letter, we present an alternative technique for acquiring the response of MEMS. Based on microwave reflectometry, the measurement method rejects parasitic crosstalk and gives access to optimal sensitivity and SNR.

The dynamics of motion of a MEMS resonator can be predicted using the 1D differential equation of a second-order system as follows:[24]

$$m_r \frac{d^2x}{dt^2} + \alpha \frac{dx}{dt} + k_r x = F_e, \tag{1}$$

where x represents the displacement of the resonator body, m_r and k_r are, respectively, the effective mass and spring constant of the resonator for the vibration mode under consideration, α is the damping coefficient, and F_e is the driving force due to the input actuation voltage. Such a modeling of a resonator is depicted in Figure 1. In the case of capacitively transduced MEMS resonators, actuation principle is electrostatic. The force is attractive and given by[25]

$$F_e = \frac{1}{2}\frac{\partial C_{in}}{\partial x}(V_{DCin} + V_{ACin})^2, \tag{2}$$

where C_{in} is the input transducer capacitance between a fixed electrode and the resonator body, and V_{DCin} and V_{ACin} are the dc and ac voltages inducing the time-varying force.

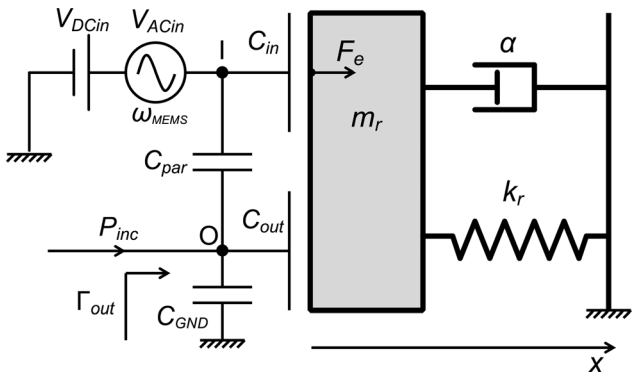

FIG. 1. Modeling of the resonator and its driving and sensing schemes. I: input port, O: output port.

Displacement sensing is usually obtained through the current flowing from the output transducer capacitance C_{out} being modulated by the resonator body vibration. The approach employed here to detect the MEMS resonator vibration is different. The concept is based on the detection of a microwave (MW) signal reflected by the output transducer impedance that is ruled by the dynamics of the resonator (Eq. (1)). In this way, the reflection coefficient is time-dependent according to the dynamics imposed by the vibration of the MEMS resonator. Although the reflection coefficient is strictly defined for a steady-state sinusoid, it can be assumed it is the case when the MW carrier frequency is much higher than the MEMS device resonance frequency. Expression (3) gives the reflection coefficient Γ_{out} neglecting capacitor parallel losses, which is a reasonable assumption at MW frequencies for the devices under study,[26]

$$\Gamma_{out} = \frac{1 - jZ_0C\omega_C}{1 + jZ_0C\omega_C} = \exp[-2j\arctan(Z_0C\omega_C)]. \quad (3)$$

Z_0 is the reference impedance (characteristic impedance of the transmission line), ω_C is the MW carrier angular frequency, and C is the capacitance of the MEMS resonator output port. Assuming small displacements of the resonator body regarding the output transducer air gap, C can be expressed as a function of x,

$$C(x) \approx C_{GND} + C_{par} + C_{out}|_{x=0} + \left.\frac{\partial C_{out}}{\partial x}\right|_{x=0} \cdot x, \quad (4)$$

where C_{out} have been defined previously, C_{par} is the parasitic input/output coupling capacitance, and C_{GND} represents the parasitic capacitance of the transducer port to the ground. From Eqs. (3) and (4), Γ_{out} is re-expressed as a function of x,

$$\Gamma_{out}(x) \approx \Gamma_0\left[1 - j\frac{2Z_0\omega_C}{1 + (Z_0C_0\omega_C)^2}\left.\frac{\partial C_{out}}{\partial x}\right|_{x=0} \cdot x\right], \quad (5)$$

where Γ_0 is the reflection coefficient of the output transducer of the MEMS resonator at equilibrium position and C_0 its static capacitance. C_0 and Γ_0 are given by

$$C_0 = C_{GND} + C_{par} + C_{out}|_{x=0}, \quad (6)$$

$$\Gamma_0 = \exp[-2j\arctan(Z_0C_0\omega_C)]. \quad (7)$$

Expression (5) shows that the vibration of the MEMS resonator gives rise to a variation of the reflection coefficient in quadrature with the main part, which can be actually perceived as a phase modulation of the reflection coefficient. The amplitude of this variation is maximum for a given value ω_{Copt} of the angular frequency of the MW carrier ω_C,

$$\omega_{Copt} = \frac{1}{C_0Z_0}. \quad (8)$$

The reference impedance is $Z_0 = 50\ \Omega$, which corresponds to the characteristic impedance of the transmission lines employed in most of measurement systems. C_0 is in the 0.1–1 pF range for MEMS resonators with micrometric dimensions, C_{par} and C_{GND} being of the order of a few hundreds of fF, and C_{out} usually comprised between 1 and 100 fF. The optimal carrier frequency is then in the 3–30 GHz range, which is actually much higher than the multi-MHz resonance frequency of MEMS resonators, as assumed previously. When the condition (8) is fulfilled, the output transducer coefficient becomes

$$\Gamma_{out}(x, \omega_{Copt}) \approx \Gamma_0(\omega_{Copt}) \cdot \left[1 - j\frac{1}{C_0}\left.\frac{\partial C_{out}}{\partial x}\right|_{x=0} \cdot x\right]. \quad (9)$$

In harmonic regime, the MEMS resonator being driven at angular frequency ω_{MEMS}, the reflected MW signal is then composed of a combination of signals at ω_C and $\omega_C \pm \omega_{MEMS}$. Information related to the resonator body displacement x is so transposed in the GHz range, which suppresses any undesirable parasitic crosstalk from the driving signal $V_{ACin}(\omega_{MEMS})$. The amplitude of the reflected MW signal at $\omega_C \pm \omega_{MEMS}$ is directly proportional to the resonator body displacement x and its power P_{MEMS} is given by

$$P_{MEMS} = P_{inc} \cdot \left[\frac{1}{C_0}\left.\frac{\partial C_{out}}{\partial x}\right|_{x=0} \cdot x\right]^2, \quad (10)$$

where P_{inc} is the incident wave power to the MEMS output transducer.

An ultimate value of the measurement resolution can be estimated assuming the thermal noise being the limit for the detection of a MW signal. At room temperature, the spectral density of noise given by k_BT is $P_{noise} = -174$ dBm/Hz. For typical values of $C_0 = 1$ pF and $P_{inc} = 1$ mW $= 0$ dBm, the detectable variation of capacitance C_{out} calculated from Eq. (10) is 2 zF/$\sqrt{\text{Hz}}$. Assuming C_{out} is a parallel plate capacitor whose static value is 0.1 pF with an air gap width of $d = 100$ nm, and neglecting fringe effects, the measurement resolution x_{min} of the MEMS resonator body displacement given by Eq. (11) is 2 fm/$\sqrt{\text{Hz}}$,

$$x_{min} = d\frac{C_0}{C_{out}|_{x=0}}\sqrt{\frac{P_{noise}}{P_{in}}}. \quad (11)$$

In a practical case, detecting the resonator vibration requires demodulating the reflected MW signal as presented hereafter. Signal losses through microwave components and extra noise added to the signals will degrade the resolution presented above.

An experimental set-up shown in Figure 2 has been implemented to demonstrate the measurement concept and performance. This measurement technique can be applied to any kind of MEMS resonator shapes like flexural beams, micro-disks or square plates, and to any vibrational modes that induce a modulation of the transducer capacitance as stated before. In the following, for the present demonstration, the device under test (DUT) consists of a silicon ring microresonator vibrating along the elliptic mode. Design considerations, fabrication, and application as force sensors of such MEMS devices have been detailed elsewhere.[18,27,28] The DUT is driven into vibration by a combination of dc and ac signals provided by a vectorial network analyzer (VNA) at angular frequency ω_{MEMS}. A MW source supplies the carrier wave at angular frequency ω_C. This incident wave passes through the coupler, the circulator, and the high pass filter. It is reflected and modulated by the impedance of the DUT output transducer according to the reflection coefficient given by Eq. (5). The circulator directs the reflected wave to the frequency mixer. A reference wave obtained from the coupler arm feeds the mixer. It is amplified and phase-shifted to obtain enough power to supply the mixer and to down-convert the components of interest at $\omega_C \pm \omega_{MEMS}$. As discussed before, they are in quadrature with respect to the main part of the reflected signal. The converted signal, proportional to the MEMS resonator body displacement, is amplified and filtered, being subsequently analyzed in magnitude and phase by the VNA receiver. When setting up the experiment, a special care has to be taken to the selection of the parts and devices. Indeed, any losses and added noise cause a decrease in the SNR and thus a loss of measurement resolution. This is particularly the case for the path of the reflected wave. The experimental set-up has been optimized to work at a MW carrier frequency of 4 GHz. The circulator, frequency mixer, and LNA are so chosen to feature insertion losses, conversion losses, and noise figure as low as possible, respectively. The DUT is probed using coplanar tips and connected to the measurement set-up using 1 m coaxial cables whose losses do not exceed 0.5 dB/m at 4 GHz. A PNA series analyzer from Agilent Technologies is used as the VNA. Other parts of the circuit are commercially available and are chosen according to the working frequency. A more detailed analysis would show that the noise of the demodulated signals is dominated by the phase noise of the MW source at ω_{MEMS} from the carrier. The source noise is actually reflected by the DUT being superimposed to the signal containing the DUT vibration information. Besides, when working at a fixed MW carrier angular frequency ω_C, measurement sensitivity may be reduced. Figure 3 shows measurement relative sensitivity as a function of the static capacitance C_0 of the transducer, which is derived from expression (5). The sensitivity is maximized when the condition (8) is met. For the chosen MW carrier frequency of 4 GHz, it is deduced that sensitivity greater than 50% of the maximum is obtained for a range of capacitance value C_0 comprised between 0.26 and 3.74 pF. This gives acceptable results in terms of expected performance. It also brings about the flexibility for measuring a great variety of MEMS resonators.

The DUT shown in Figure 2 is used in the experiments. The silicon ring inner radius, outer radius, thickness, and effective spring constant are 15 μm, 30 μm, 5 μm, and 400 kN/m, respectively. The resonance frequency of the ring elliptic mode is expected at around 22.5 MHz. The static capacitance value of the DUT ports being measured by standard techniques is $C_0 = 0.6$ pF. The static value of the transducer capacitances C_{in} and C_{out} neglecting fringe effects are calculated to be 18 fF, considering a transducer air gap $d = 70$ nm measured from scanning electron microscopy images. In the following, the MW carrier frequency is 4 GHz and the MW incident power to the DUT output port is $P_{inc} = 4$ dBm. Figure 4 shows the frequency response of the DUT when driven close to its resonance frequency. Figures 4(a) and 4(b) are the standard reflection and transmission parameters measured by a VNA. Figures 4(c) and 4(d) show the frequency response in magnitude and phase obtained with the microwave reflectometry technique. The magnitude signal shows a nice Lorentzian behavior, the resonance frequency and quality factor being 22.375 MHz and 1800, respectively. The 180° phase rotation confirms negligible effects of any parasitic input/output parasitic coupling signal

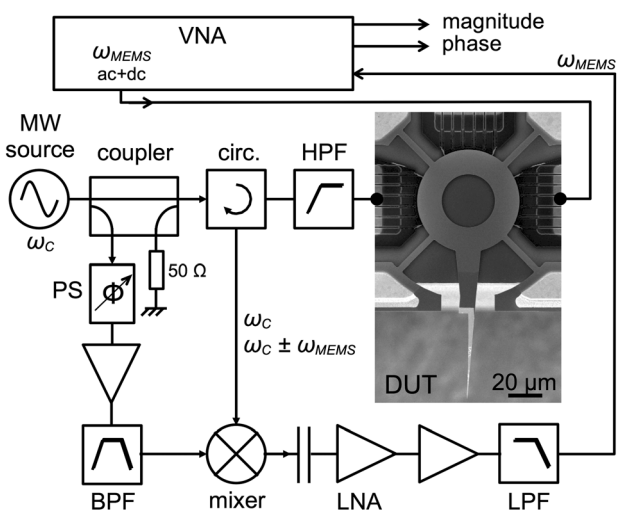

FIG. 2. Block diagram of the experimental set-up used to measure MEMS resonator vibration with the proposed microwave reflectometry technique. The (DUT) is driven into vibration by the (VNA) using ac + dc signal at the angular frequency ω_{MEMS}. (PS: phase shifter, circ.: circulator, HPF: high pass filter, BPF: band pass filter, LPF: low pass filter, LNA: low noise amplifier.)

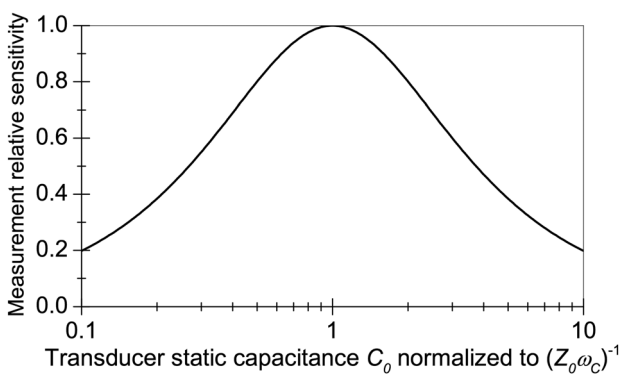

FIG. 3. Relative sensitivity of the microwave measurement technique for a given carrier frequency ω_C as a function of the static capacitance of the output transducer.

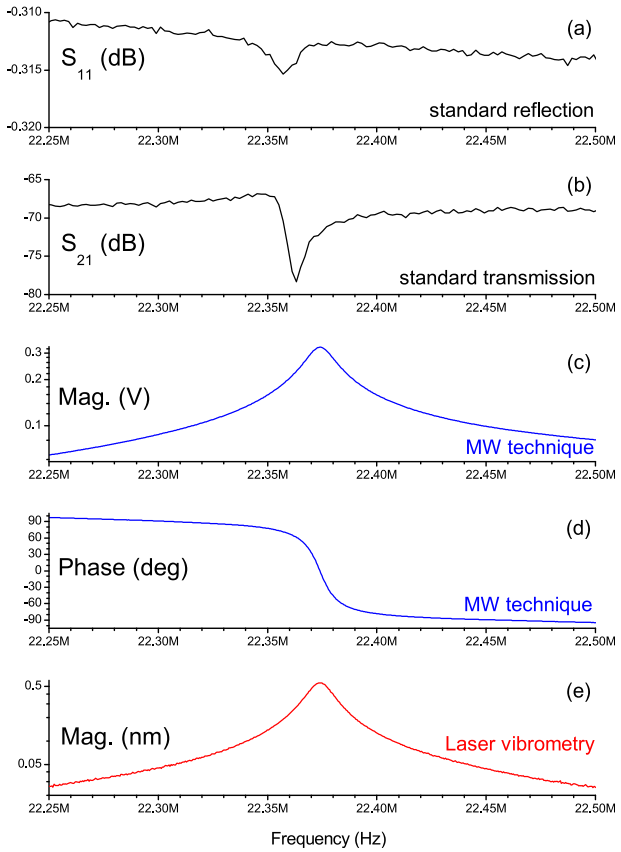

FIG. 4. Frequency response of the MEMS device. $V_{ACin} = 0.45$ V corresponding to 0 dBm source power applied to the high impedance of the DUT input transducer. Measurement bandwidth: 100 Hz. (a) and (b): standard reflection and transmission measurements with 10 V DC bias. (c) and (d): magnitude and phase measurements obtained with the microwave reflectometry technique at $V_{DCin} = 2$ V. (e): Laser Doppler vibrometry measurement of the mechanical amplitude acquired simultaneously with (c) and (d).

floor. The slight shift in the resonance frequency is ascribed to the spring softening due to the different DC bias applied. Figure 4(e) shows the laser Doppler vibrometry (LDV) measurement of the mechanical amplitude acquired simultaneously with Figs. 4(c) and 4(d). In order to estimate the noise level and resolution, further experiments have been carried out regarding the measurement dynamics. Figure 5(a) shows the magnitude signal in the same condition as in Figures 4(c) and 4(d). The noise floor, that is visible in Figure 5(b), is obtained by switching off the VNA source (*i.e.*, $V_{ACin} = 0$ V), or, in other words, by suppressing the DUT actuation. Noise level is then measured to be 3 μV for a 1 Hz measurement bandwidth (BW), which corresponds to a noise density of 3 μV/$\sqrt{\text{Hz}}$ at the output of the measurement set-up. In the experimental conditions of Figure 5(a) and at the resonance frequency, the SNR is about 100 dB (BW = 1 Hz), and it is calculated from Eqs. (1) and (2) that the DUT vibration amplitude is 1 nm.[29] The LDV measures 0.6 nm but this value can be underestimated since the LDV bandwidth is only certified up to 20 MHz. Considering the noise floor of Figure 5(b) as the detection limit of the DUT vibration, the measurement resolution in amplitude is then between 6 to 10 fm/$\sqrt{\text{Hz}}$. This value is greater than the ultimate one calculated from Eq. (11) that gives $x_{min} = 3$ fm/$\sqrt{\text{Hz}}$. As mentioned before, the discrepancy is explained by extra noise added by the measurement set-up and by the MW carrier frequency

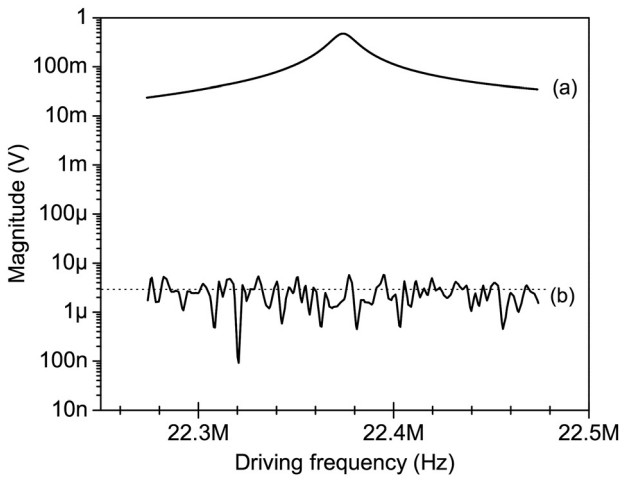

FIG. 5. Frequency response in magnitude of the MEMS device using microwave reflectometry. $V_{DCin} = 2$ V. (a) $V_{ACin} = 0.45$ V corresponding to 0 dBm VNA source power, (b) $V_{ACin} = 0$ V corresponding to VNA source power off, measurement bandwidth: 1 Hz.

that does not perfectly match condition (8). As the capacitance variations are concerned, it is deduced from these results that a resolution of 1.8 to 3 zF/$\sqrt{\text{Hz}}$ is experimentally achieved for the studied DUT. Using the same procedure, i.e., by suppressing the DUT actuation, the SNR was estimated for standard transmission measurements to 50 dB and, for LDV measurement to 80 dB (BW = 1 Hz).

In conclusion, a measurement method using microwave reflectometry has been presented for the characterization of MEMS resonators based on the capacitive transduction. The reflection coefficient associated with the transducer capacitance has been studied showing that the sensitivity is maximized for a given microwave frequency. The study has also pointed out that considering the thermal noise as the ultimate detection limit, measurement resolution in the femtometer range can be then expected. An experimental set-up has been described and implemented to characterize a device based on a silicon ring vibrating along the elliptic mode at 22.375 MHz. The measured signal is directly proportional to the resonator body displacement and parasitic input/output coupling signals are rejected. A large signal-to-noise ratio up to 100 dB has been evidenced and a 10 fm/$\sqrt{\text{Hz}}$ resolution has been experimentally achieved, which proves the effectiveness of concept. Such a performance level is comparable to the one of standard optical interferometry, which paves the way for the use of the capacitive transduction for high performance vibrating sensors.

This work was supported by Agilent Program for University Research and received funding from the European Community's Seventh Framework Program FP7/2007-2013 under Grant 210078. The authors would like to acknowledge the IEMN cleanroom and electrical characterization staff for their constant support.

[1]S. J. Sherman, W. K. Tsang, T. A. Core, R. S. Payne, D. E. Quinn, K. H.-L. Chau, J. A. Farash, and S. K. Baum, in *Proceedings of International Electron Devices Meeting, San Francisco* (IEEE, 1992), p. 501.
[2]M. Lutz, W. Golderer, J. Gerstenmeier, J. Marek, B. Maihofer, S. Mahler, H. Munzel, and U. Bischof, in *Proceedings of the International Conference*

on Solid-State Sensors, Actuators and Microsystems, Chicago (IEEE, 1997), p. 847.
[3]P. F. Van Kessel, L. J. Hornbeck, R. E. Meier, and M. R. Douglas, Proc. IEEE **86**(8), 1687 (1998).
[4]G. M. Rebeiz and J. B. Muldavin, IEEE Microw. Mag. **2**(4), 59 (2001).
[5]C. Yamahata, D. Collard, B. Legrand, T. Takekawa, M. Kumemura, G. Hashiguchi, and H. Fujita, J. Microelectromech. Syst. **17**(3), 623 (2008).
[6]W. C. Tang, T.-C. H. Nguyen, and R. T. Howe, Sens. Actuators **20**(1–2), 25 (1989).
[7]J. R. Clark, W. T. Hsu, and C. T.-C. Nguyen, in *Proceedings of the International Electron Devices Meeting, San Francisco* (IEEE, 2000), p. 493.
[8]S. Pourkamali, Z. Hao, and F. Ayazi, J. Microelectromech. Syst. **13**, 1054 (2004).
[9]M. Sworowski, F. Neuilly, B. Legrand, A. Summanwar, P. Philippe, and L. Buchaillot, IEEE Electron Device Lett. **31**(1), 23 (2010).
[10]G. Stemme, J. Micromech. Microeng. **1**(2), 113 (1991).
[11]N. Yazdi, F. Ayazi, and K. Najafi, Proc. IEEE **86**(8), 1640 (1998).
[12]B. Ilic, H. G. Craighead, S. Krylov, W. Senaratne, C. Ober, and P. Neuzil, J. Appl. Phys. **95**(7), 3694 (2004).
[13]Y. T. Yang, C. Callegari, X. L. Feng, K. L. Ekinci, and M. L. Roukes, Nano lett. **6**(4), 583 (2006).
[14]R. T. Howe and R. S. Muller, in *Proceedings of the International Electron Devices Meeting, San Francisco* (IEEE, 1984), p. 213.
[15]T. P. Burg and S. R. Manalis, Appl. Phys. Lett. **83**(13), 2698 (2003).
[16]J. L. Arlett, E. B. Myers, and M. L. Roukes, Nat. Nanotechnol. **6**, 203 (2011).
[17]S. C. Minne, S. R. Manalis, and C. F. Quate, Appl. Phys. Lett. **67**(26), 3918 (1995).
[18]E. Algré, Z. Xiong, M. Faucher, B. Walter, L. Buchaillot, and B. Legrand, J. Microelectromech. Syst. **21**(2), 385 (2012).
[19]D. J. Bell, T. J. Lu, N. A. Fleck, and S. M. Spearing, J. Micromech. Microeng. **15**(7), S153 (2005).
[20]W. T. Hsu, J. R. Clark, and C. T.-C. Nguyen, in *Proceedings of the International Conference on MicroElectroMechanical Systems, Interlaken* (IEEE, 2001), p. 349.
[21]J. R. Clark, W. T. Hsu, M. A. Abdelmoneum, and C. T.-C. Nguyen, J. Microelectromech. Syst. **14**(6), 1298 (2005).
[22]P. A. Truitt, J. B. Hertzberg, C. C. Huang, K. L. Ekinci, and K. C. Schwab, Nano Lett. **7**(1), 120 (2007).
[23]C. Durand, F. Casset, P. Renaux, N. Abelé, B. Legrand, D. Renaud, E. Ollier, P. Ancey, A. M. Ionescu, and L. Buchaillot, IEEE Electron Device Lett. **29**(5), 494 (2008).
[24]H. A. C. Tilmans, J. Micromech. Microeng. **7**(4), 285 (1997).
[25]S. D. Senturia, *Microsystem Design* (Kluwer Academic, Boston, 2002).
[26]A. S. Ramo, J. R. Whinnery, and T. Van Duzer, *Fields and Waves in Communication Electronics* (Wiley, New York, 1994).
[27]B. Walter, M. Faucher, E. Algré, B. Legrand, R. Boisgard, J. P. Aimé, and L. Buchaillot, J. Micromech. Microeng. **19**(11), 115009 (2009).
[28]B. Walter, M. Faucher, E. Mairiaux, Z. Xiong, L. Buchaillot, and B. Legrand, in *Proceedings of the International Conference on MicroElectroMechanical Systems, Cancun* (IEEE, 2011), p. 517.
[29]Calculation of the electrostatic force assumes a parallel plate capacitor, neglects fringe effects and takes into account a correction due to the DUT vibration mode shape.